Available online at www.sciencedirect.com

SciVerse ScienceDirect

Nuclear Physics A 890–891 (2012) 29–49

NUCLEAR PHYSICS A

www.elsevier.com/locate/nuclphysa

Investigation of spectral statistics of nuclear systems by maximum likelihood estimation method

M.A. Jafarizadeh [a,b], N. Fouladi [c], H. Sabri [c,*], B. Rashidian Maleki [c]

[a] *Department of Theoretical Physics and Astrophysics, University of Tabriz, Tabriz 51664, Iran*
[b] *Research Institute for Fundamental Sciences, Tabriz 51664, Iran*
[c] *Department of Nuclear Physics, University of Tabriz, Tabriz 51664, Iran*

Received 6 April 2012; received in revised form 27 June 2012; accepted 16 July 2012

Available online 20 July 2012

Abstract

In this paper, maximum likelihood estimation technique is employed to consider the spectral statistics of nuclear systems in the nearest neighbor spacing distribution framework. With using the available empirical data, the spectral statistics of different sequences are analyzed. The ML-based estimated values propose more regular dynamics and also minimum uncertainties (variations very close to CRLB) in compare to other estimation methods. Also, the efficiencies of considered distribution functions are examined where suggest the least CRLB for Brody distribution.

Keywords: Maximum Likelihood Estimation (MLE); Spectral statistics; Interacting Boson Model (IBM); Cramer–Rao Lower Bound (CRLB)

1. Introduction

The investigations of spectral statistics and non-linear dynamics in different systems are recently receiving considerable attentions. In common analyses [1,2], the fluctuation properties of quantum system's spectra are compared with the prediction of Random Matrix Theory (RMT). This model describes a chaotic system by an ensemble of random matrices subject only to the symmetry restrictions. Systems with time reversal symmetry such as atomic nuclei are described by Gaussian Orthogonal Ensemble (GOE). On the other hand, systems whose classical dynamics

* Corresponding author.
E-mail addresses: jafarizadeh@tabrizu.ac.ir (M.A. Jafarizadeh), h-sabri@tabrizu.ac.ir (H. Sabri).

0375-9474/$ – see front matter
http://dx.doi.org/10.1016/j.nuclphysa.2012.07.007

are everywhere rigorous in the phase space, are well characterized by Poisson distribution [3–6]. The statistical analyses which accomplished on different nuclear systems' spectra, proposed an intermediate behavior between these two extremes for considered systems.

Different statistics [1–3] have been employed to describe the statistical situations of systems in related to these limits while the Nearest Neighbor Spacing Distribution (NNSD) is the observable most commonly used to analyze the short-range fluctuation properties of nuclear spectra. In NNSD framework [2–5], a Least Square Fit (LSF) have been carried out to compare the spacings of each sequences with some well-known distributions such as Brody and etc [7–10] while the value of every distribution's parameter(s) describes the deviation to regular or chaotic dynamics. The great uncertainties and also some unacceptable results in some sequences (particularly with small size of data) have been interpreted in this approach [3–5].

On the other hand, the LSF is one of the widely used estimation methods more well known than the other parametric estimation methods included Maximum Likelihood Estimation (MLE) or Bayesian Estimation methods (BEM) [11]. Although, as presented in Ref. [12], the LSF is really equivalent to producing a maximum likelihood procedure in the variables estimating which are linearly related to some Gaussian case. Therefore, one can expect, in sequences where the LSF method yields estimation very close to GOE (chaotic) limit, other estimation methods, those with more precise in compare to LSF which yield estimation more close to real distribution, predict more regular dynamics.

In this paper, we employed the MLE technique [11–17] to estimate the parameter(s) of all considered distributions (Brody, Berry–Robnik and Abul-Magd distributions). Also, to obtain the uncertainties of estimated values, we used the Cramer–Rao Lower Bound (CRLB) [11] which is the common method to determine the uncertainties of unbiased estimators (as mentioned in Ref. [15], the MLE method achieves the lowest CRLB).

To compare the ML-based estimated statistics with the predictions of other parametric estimation techniques, we employed sequences introduced in Refs. [3,18] where description have been carried out by LSF technique. The MLE method proposes similar spectral statistics in different sequences but with more precision (the accuracies very close to CRLB) and also less chaotic dynamics in compare to other methods.

To propose a physical meaning for the estimated values, similar to procedure have been concerned in Ref. [18], we estimated the parameter of Berry–Robnik distribution in sequences prepared by nuclei classified in different mass regions which have definite quadrupole deformation parameter "β_2". The ML-based estimated values confirm previous predictions with again less chaoticity in compare to LSF-based estimated values.

Also, with employing the MLE technique, the parameter of Abul-Magd's distribution estimated in sequences prepared by oblate and prolate nuclei. The ML-based estimated values suggest same spectral statistics (similar to the predictions of Refs. [19,20] where BEM have been used) with more regularities and more precisions.

With using all the available experimental data [21–25], namely 2^+ and 4^+ levels of nuclei in which the spin–parity J^π assignment of at least five consecutive levels are definite, the spectral statistics of nuclei provide empirical evidences for three dynamical symmetry limits and transitional regions of Interacting Boson Model (IBM) [26,27] analyzed. The ML-based estimated values, confirm theoretical predictions, namely, suggest more regular dynamics for nuclei characterize dynamical symmetry limits (particularly, nuclei with U(5) dynamical symmetry) and also less regular dynamics by nuclei localized in the transitional regions [29–31].

Finally, to compare the efficiencies of different distributions in the same sequences, we determined CRLBs for all considered distributions where Brody distribution has the least CRLB.

The paper is arranged as follows. Section 2 briefly summarizes the statistical approaches included unfolding process, well-known distributions, MLE and CRLB techniques. In Section 3, we present the ML-based considered relations for all distributions. Section 4, contains the numerical results obtained by applying the MLE method to different sequences. Section 5 is devoted to comparison of MLE method with LSF one, based on results given in Section 4. The paper ends with appendices containing the details and related calculations of Brody, Berry–Robnik and Abul-Magd distributions and CRLBs.

2. Statistical analysis

2.1. Nearest Neighbor Spacing Distribution (NNSD)

The spectral fluctuations of low-lying nuclear levels have been considered by different statistics such as Nearest Neighbor Spacing Distribution (NNSD) [1], linear coefficients between adjacent spacing [3] and Dyson–Mehta $\Delta_3(L)$ statistics [3–5] which based on the comparison of statistical properties of nuclear spectra with the predictions of Random Matrix Theory (RMT). The NNSD, or $P(s)$ functions, is the observable most commonly used to analyze the short-range fluctuation properties in the nuclear spectra. On the other hand, the NNSD statistics would perform by complete (few or no missing levels) and pure (few or no unknown spin–parities) level scheme [3] where these conditions are available for a limited number of nuclei. Therefore, to obtain the statistically relevant samples, we in need to combine different level schemes to construct sequences. To compare the different sequences to each other, each set of energy levels must be converted to a set of normalized spacing, namely, each sequence must be unfolded. The unfolding process has been described in detail in Ref. [3]. Here, we briefly outline the basic ansatz and summarize the results. To unfold our spectrum, we had to use some levels with same symmetry. This requirement is equivalent with the use of levels with same total quantum number (J) and same parity. Firstly we consider the number of the levels below E and write it as [3]

$$N(E) = \int_0^E \rho(E)\,\mathrm{d}E = e^{\frac{E-E_0}{T}} - e^{-\frac{E_0}{T}} + N_0. \tag{2.1}$$

N_0 establishes the number of levels with energies less than zero and must be assume as zero. The best fit to $N(E)$ ($\equiv F(E)$) would be carried while a correct set of energies is prepared by means of

$$E_i' = E_{\min} + \frac{F(E_i) - F(E_{\min})}{F(E_{\max}) - F(E_{\min})}(E_{\max} - E_{\min}), \tag{2.2}$$

both $E_{\max}$ and $E_{\min}$ remain unchanged with this transformation. These transformed energies should now display on average a constant level density. The normalized spacing used in the determination of NNS distributions are given by

$$S_i = E_{i+1}' - E_i', \qquad s_i = \frac{S_i}{D} \tag{2.3}$$

where D is the average of the spacing between corrected energy levels. Distribution $P(s)$ will be in such a way in which $P(s)\,\mathrm{d}s$ is the probability for the s_i to lie within the infinitesimal interval $[s, s + \mathrm{d}s]$. For nuclear systems with time reversal symmetry while spectral spacing follows Gaussian Orthogonal Ensemble (GOE) statistics, the NNS probability distribution function is well approximated by Wigner distribution [1,2]

$$P(s) = \frac{1}{2}\pi s e^{-\frac{\pi s^2}{4}}, \tag{2.4}$$

while exhibits the chaotic properties of spectra. On the other hand, the NNSD of systems with regular dynamics is generically represented by Poisson distribution

$$P(s) = e^{-s}. \tag{2.5}$$

Different investigations have been accomplished on nuclear system's spectra, proposed intermediate performance of spectral statistics between these two regular and chaotic limits [3–6]. Different distributions functions (with one or more parameters) were suggested to describe the intermediate situation of considered systems. One of popular distribution is Brody distribution [7]

$$P(s) = b(1+q)s^q e^{-bs^{q+1}}, \quad b = \left[\Gamma\left(\frac{2+q}{1+q}\right)\right]^{q+1}. \tag{2.6}$$

Considers a power-law level repulsion and interpolates between the Poisson ($q = 0$) and Wigner ($q = 1$) limits. Another distribution which proposed by Berry–Robnik is derived by assuming that, the energy level spectrum is a product of the superposition of independent subspectra, which are contributed respectively from localized eigenfunctions into invariant (disjoint) phase space [8]

$$P(s) = \left[q + \frac{1}{2}\pi(1-q)s\right]e^{-qs-\frac{1}{4}\pi(1-q)s^2}, \tag{2.7}$$

where exhibits Poisson and GOE limits by $q = 1$ and 0, respectively. Another distribution which is appropriate to use, is distribution proposed by the Rosenzweig and Porter random matrix model. The exact form of this model is complicated and its simpler form is proposed by Abul-Magd et al. in Refs. [9,10] as:

$$P(s,q) = \left[1 - q + q(0.7 + 0.3q)\frac{\pi s}{2}\right]\exp\left(-(1-q)s - q(0.7+0.3q)\frac{\pi s^2}{4}\right), \tag{2.8}$$

where interpolates between Poisson ($q = 0$) and Wigner ($q = 1$) limits. In common descriptions, the parameter(s) of considered distribution while exhibits the chaoticity degree of spectra, is determined via the best fit obtained by LSF technique. The LSF is on firm theoretical grounds when it can reasonably be assumed that the deviations of the observations from the expectations of the true theory are independently, identically and normally distributed. Therefore, one can expect a deviation to chaotic dynamics by prediction of LSF. To avoid these problems, Abul-Magd et al. [9,10] have employed the BEM technique in their analyses where have achieved more precision and also more regularities for considered systems in compare to the predictions of LSF. In the following, we would employ the MLE technique to describe the spectral statistics of considered systems with more accuracy.

2.2. Maximum Likelihood Estimation (MLE)

The LSF is one of the parametric estimation methods which the present use is subjective but some disadvantages such as a deviation to GOE limit and also great uncertainties in the estimation processes for sequences with small size of data have been interpreted. Some suggestions have been advised to overcome these problems while the best one is Maximum Likelihood (ML) method. The ML method has been described in detail in Refs. [11–16]. Here, we briefly outline

the basic ansatz and summarize the results. The likelihood function for the probability distribution function $f(x;\theta) = f(x_1,\ldots,x_n;\theta)$ of random variables $(X_1,\ldots,X_n)$ (both discrete and continuous variables), is defined as [11–16]

$$L(\theta) = f(x;\theta) = f(x_1,\ldots,x_n;\theta). \tag{2.9}$$

That is the chance function for observing variables $(x_1,\ldots,x_n)$ in order to obtaining a correct choice of θ. If $\theta_{ML} = s(x_1,\ldots,x_n)$ indicates the maximum value of function $L(\theta)$, namely

$$L(\theta_{ML}) = \operatorname{Max} L(\theta). \tag{2.10}$$

Thus, the likelihood estimator of θ is defined as

$$\Theta_{ML} = s(X_1,\ldots,X_n). \tag{2.11}$$

Therefore θ_{ML} is the estimate or MLE suggestion for θ. In the estimation procedure of θ, we would consider the fact that $L(\theta)$ and $\ln L(\theta)$ have maximum value for the same θ. Consistency, namely, the estimator converges to the value that has been estimated and also more efficiency which means, it would reach to the lower bound of Cramer–Rao have been considered as advantages of this technique. These mean, asymptotic mean squared errors of any asymptotically unbiased estimators wouldn't lower than those of MLE. To describe the uncertainties in the estimation procedures, we would use the Cramer–Rao lower bound which is a limit for the variance would be attained by an unbiased estimator.

2.3. Cramer–Rao Lower Bound (CRLB)

In the estimation theory and statistical applications, the Cramer–Rao lower bound (CRLB) measures how close this estimator's variance comes to this lower bound. Suppose θ is an unknown deterministic parameter which is to be estimated from measurements of x and also suppose that its corresponding distribution probability density function is $f(x;\theta)$. Inverse of the Fisher information bounds the variance of any unbiased estimator θ of θ as fallow [11,15]:

$$\operatorname{var}(\hat{\theta}) \geqslant \frac{1}{MF(\theta)}, \tag{2.12}$$

where M is the sample size and Fisher information $F(\theta)$ is defined as follows:

$$F(\theta) = E\left[\left(\frac{\partial \ln f(x;\theta)}{\theta}\right)^2\right],$$

$$f(x;\theta) \equiv P(s) \quad \Rightarrow \quad F(\theta) = \sum \frac{1}{P(s)}\left[\frac{\mathrm{d}\ln P(s)}{\mathrm{d}\theta}\right]^2.$$

The expression (2.12) is called the Cramer–Rao inequality. The scalar quantity $\frac{1}{MF(\theta)}$ is the CRLB on the variances of unbiased estimators of $f(x;\theta)$ $(\equiv P(s))$.

2.4. The Cramer–Rao Lower Bound for vector functions of vector parameters

One can assume a parameter column vector in order to extending the Cramer–Rao bound into multiple parameters,

$$\theta = [\theta_1, \theta_2, \ldots, \theta_d]^T \in \mathbb{R}^d.$$

With probability density function of $f(x;\theta)$ which satisfies the regularity condition. On the other hand, Fisher information matrix would be a $d\times d$ matrix with element $F_{m,k}$ that is defined as [11]

$$F_{m,k}=E\left[\frac{\mathrm{d}}{\mathrm{d}\theta_m}\log f(x;\theta)\frac{\mathrm{d}}{\mathrm{d}\theta_k}\log f(x;\theta)\right].$$

Assume $T(X)$ be an estimator of any vector function of parameters, namely $T(X)=(T_1(X),\ldots,T_N(X))^T$, and denote its expectation vector $E[T(X)]$ by $\rho(\theta)$, consequently, the Cramer–Rao bound shows that the covariance matrix $T(X)$ satisfies as [11]

$$\mathrm{cov}_\theta\big(T(X)\big)\geqslant\frac{\partial\rho(\theta)}{\partial\theta^T}\big[F(\theta)\big]^{-1}\frac{\partial\rho^T(\theta)}{\partial\theta}. \tag{2.13}$$

Similar to scalar one (2.12), the expression (2.13) is called the Cramer–Rao inequality and quantity $\frac{\partial\rho(\theta)}{\partial\theta^T}[F(\theta)]^{-1}\frac{\partial\rho^T(\theta)}{\partial\theta}$ is the CRLB. The difference between the traces of left and right sides of Eq. (2.13) will be used to describe the variation (decreasing) of uncertainties for estimated parameters during the iterations.

3. The MLE-based relations for parameter(s) of considered distribution functions

Now we are proceeding to determine the parameters of the above introduced distributions functions via the MLE technique.

3.1. Brody distribution

Due to some problems concerned in the maximizing the likelihood function containing the Gamma functions, we propose a generalized Brody distribution with two parameters b and q as:

$$P(s)=b(1+q)s^q e^{-bs^{q+1}}, \tag{3.1}$$

where it reduces to Brody one by choosing $b=[\Gamma(\frac{2+q}{1+q})]^{q+1}$. In the following, namely Fig. 7, we would present a closer corresponding between our suggestion and main definition of Brody distribution. Now, in order to estimate the parameters b and q, we need to introduce the corresponding maximum likelihood estimators. To this aim, we try to use the products of the generalized Brody distribution functions as a likelihood function [11], namely

$$L(q,b)=\prod_{i=1}^{n}b(1+q)s_i^q e^{-bs_i^{q+1}}=\big[b(1+q)\big]^n\prod_{i=1}^{n}s_i^q e^{-b\sum s_i^{q+1}}. \tag{3.2}$$

Then, taking the derivative of the log of likelihood function (3.2) with respect to the parameters "q" and "b" and setting them to zero, i.e., maximizing likelihood function, we obtain the following pair of implicit equations for the required estimators:

$$f_1:\quad \frac{1}{n}\sum s_i^{q+1}-\frac{1}{b}\quad\text{for } b, \tag{3.3}$$

$$f_2:\quad \frac{b}{n}\sum\ln s_i s_i^{q+1}-\frac{1}{n}\sum\ln s_i-\frac{1}{1+q}\quad\text{for } q. \tag{3.4}$$

Now, the parameters b and q can be estimated by high precision via solving above equations by Newton–Raphson iteration method [11] (full details presented in Appendix A), where the difference between the traces of left- and right-hand sides of Eq. (2.13) (see Appendix B for more details) is used to see the decreasing of the variation of uncertainties for estimated parameters during the iterations.

3.2. Berry–Robnik distribution

We can repeat the above mentioned process for Berry–Robnik distribution [8]

$$P(s) = \left[q + \frac{1}{2}\pi(1-q)s\right]e^{-qs-\frac{1}{4}\pi(1-q)s^2}. \tag{3.5}$$

In order to estimate the parameter of distribution, likelihood function assumed as products of all $P(s)$ functions

$$L(q) = \prod_{i=1}^{n} P(s_i) = \prod_{i=1}^{n}\left[q + \frac{1}{2}\pi(1-q)s_i\right]e^{-qs_i-\frac{1}{4}\pi(1-q)s_i^2}. \tag{3.6}$$

Then, taking the derivative of the log of likelihood function (3.6) with respect to its parameter (q) and set it to zero, i.e., maximizing likelihood function, we obtain the following relation for desired estimator (see Appendix C for more details)

$$f: \quad \sum \frac{1-\frac{1}{2}\pi s_i}{q+\frac{1}{2}\pi(1-q)s_i} - \sum\left(s_i - \frac{1}{4}\pi s_i^2\right). \tag{3.7}$$

We can estimate "q" by high accuracy via solving the above equation by Newton–Raphson method. Also we would use the difference of both sides of Eq. (2.12) to obtain the decreasing of uncertainties for estimated values.

3.3. Abul-Magd's distribution

This distribution similar to Berry–Robnik distribution, considers one parameter to interpolates between regular and chaotic limits, namely;

$$P(s,q) = \left[1-q+q(0.7+0.3q)\frac{\pi s}{2}\right]\exp\left(-(1-q)s - q(0.7+0.3q)\frac{\pi s^2}{4}\right).$$

As previous case, we can prepare likelihood function to estimate "q" by products of all $P(s,q)$'s

$$L(q) = \prod_{i=1}^{n} P(s_i) = \prod_{i=1}^{n}\left[1-q+q(0.7+0.3q)\frac{\pi s_i}{2}\right]e^{-(1-q)s_i - q(0.7+0.3q)\frac{\pi s_i^2}{4}}. \tag{3.8}$$

With setting zero the derivative of the log of likelihood function (3.8) with respect to its parameter "q", i.e., maximizing likelihood function, we obtain the following relation for required estimator (see Appendix D for more details)

$$f: \quad \sum \frac{-1+(0.7+0.6q)\frac{\pi s_i}{2}}{[1-q+q(0.7+0.3q)\frac{\pi s_i}{2}]} + \sum\left[s_i - (0.7+0.6q)\frac{\pi s_i^2}{4}\right]. \tag{3.9}$$

We must use Newton–Raphson iteration method to estimate "q" (see Appendix D for more details), and also as previous case, we can use the difference of right and left sides of (2.12) to obtain decreasing of uncertainties for our estimated values.

Table 1
The LSF-based estimated values of Brody distribution's parameter "q" in different sequences taken from Ref. [3].

Sequence	All	Even–even	Even–even $(0^+, 3^+)$	Even–even $(2^+, 4^+)$	Even–even not $(2^+, 4^+)$	Odd mass	Odd–Odd
All	0.43 ± 0.05	0.42 ± 0.08	0.56 ± 0.20	0.34 ± 0.10	0.56 ± 0.13	0.40 ± 0.10	0.44 ± 0.07
Spherical	0.60 ± 0.08	0.55 ± 0.11	0.52 ± 0.21	0.52 ± 0.15	0.57 ± 0.16	1.06 ± 0.39	0.60 ± 0.12
Deformed	0.30 ± 0.06	0.26 ± 0.11	0.74 ± 0.52	0.16 ± 0.13	0.51 ± 0.21	0.32 ± 0.10	0.31 ± 0.09
$0 < A \leqslant 50$	0.72 ± 0.16	0.67 ± 0.25		0.62 ± 0.25			0.64 ± 0.21
$50 < A \leqslant 100$	0.88 ± 0.41						1.04 ± 0.67
$100 < A \leqslant 150$	0.55 ± 0.11	0.62 ± 0.16	0.46 ± 0.22	0.65 ± 0.27	0.59 ± 0.19		0.47 ± 0.15
$150 < A \leqslant 180$	0.33 ± 0.07	0.26 ± 0.11	0.74 ± 0.52	0.13 ± 0.14	0.54 ± 0.22	0.36 ± 0.14	0.36 ± 0.11
$180 < A \leqslant 210$	0.43 ± 0.17	0.30 ± 0.18		0.16 ± 0.24			1.02 ± 0.55
$230 < A$	0.24 ± 0.11	0.27 ± 0.32				0.27 ± 0.16	0.20 ± 0.16

Table 2
The ML-based estimated values of Brody distribution's parameter "q" in the similar sequences have been used in Table 1.

Sequence	All	Even–even	Even–even $(0^+, 3^+)$	Even–even $(2^+, 4^+)$	Even–even not $(2^+, 4^+)$	Odd mass	Odd–Odd
All	0.20 ± 0.03	0.19 ± 0.03	0.20 ± 0.07	0.18 ± 0.02	0.25 ± 0.02	0.17 ± 0.03	0.24 ± 0.02
Spherical	0.31 ± 0.03	0.28 ± 0.06	0.21 ± 0.09	0.28 ± 0.04	0.26 ± 0.03	0.47 ± 0.06	0.30 ± 0.03
Deformed	0.19 ± 0.02	0.14 ± 0.04	0.37 ± 0.05	0.12 ± 0.03	0.20 ± 0.05	0.13 ± 0.07	0.19 ± 0.07
$0 < A \leqslant 50$	0.28 ± 0.04	0.23 ± 0.08		0.34 ± 0.05			0.35 ± 0.05
$50 < A \leqslant 100$	0.37 ± 0.07						0.61 ± 0.11
$100 < A \leqslant 150$	0.19 ± 0.05	0.19 ± 0.04	0.27 ± 0.06	0.37 ± 0.08	0.25 ± 0.04		0.29 ± 0.02
$150 < A \leqslant 180$	0.11 ± 0.03	0.11 ± 0.02	0.31 ± 0.11	0.08 ± 0.02	0.21 ± 0.06	0.21 ± 0.02	0.23 ± 0.03
$180 < A \leqslant 210$	0.14 ± 0.04	0.14 ± 0.05		0.11 ± 0.06			0.41 ± 0.10
$230 < A$	0.09 ± 0.02	0.12 ± 0.09				0.14 ± 0.03	0.18 ± 0.03

4. MLE parameter estimation of Brody, Berry–Robnik and Abul-Magd distributions from experimental data and its comparison with other methods

As mentioned in previous sections, we expect, the estimated values by MLE method yield accuracies which are closer to CRLBs. To this aim, we apply the MLE method in estimating the parameter of Brody distribution by using the sequences introduced in Ref. [3]. These sequences constructed of empirical data for levels with definite spin–parity of nuclei given in Table 1 of Ref. [3] obtained by applying unfolding processes.

Since, the investigation of the majority of short sequences yields an overestimation about the degree of chaoticity measured by the values of different distributions parameters [9], therefore, we wouldn't concentrate only on the implicit values of them and examine a comparison between the amounts while the smallest value (in Brody and Abul-Magd distributions) explains more regular dynamics and vice versa.

The estimated values for Brody distribution's parameter corresponding to these sequences are listed in Tables 1 and 2, respectively, where the first one is obtained by LSF method while the second one estimated by MLE method. In MLE case, we have followed the prescription explained in Section 3.1, namely, the ML-based estimated parameters correspond to the converging values of iterations (A.4) and (A.5), where as an initial value, we have chosen the values of parameters obtained by LSF method given in Table 1. The ML-based estimated parameters display reduction

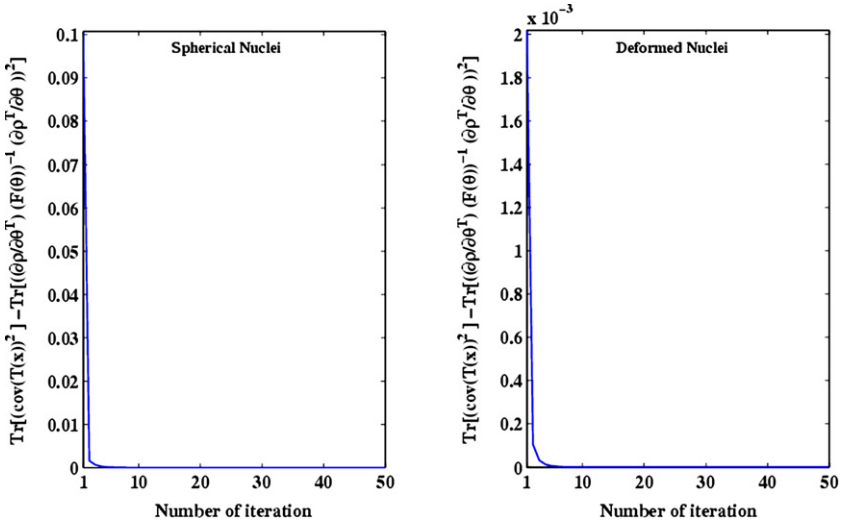

Fig. 1. (Color online.) The variations of CRLBs in the iteration processes for sequences prepared by all spherical and deformed nuclei taken from Table 1 of Ref. [3]. Since the initial values in the estimation procedure obtained by LSF method and therefore, the first points of these curves display their uncertainties where the decline of curves in the following suggest reduction of uncertainties for ML-based estimated values, i.e. propose estimator's variance very close to CRLB. Brody distribution has used in these estimation procedures.

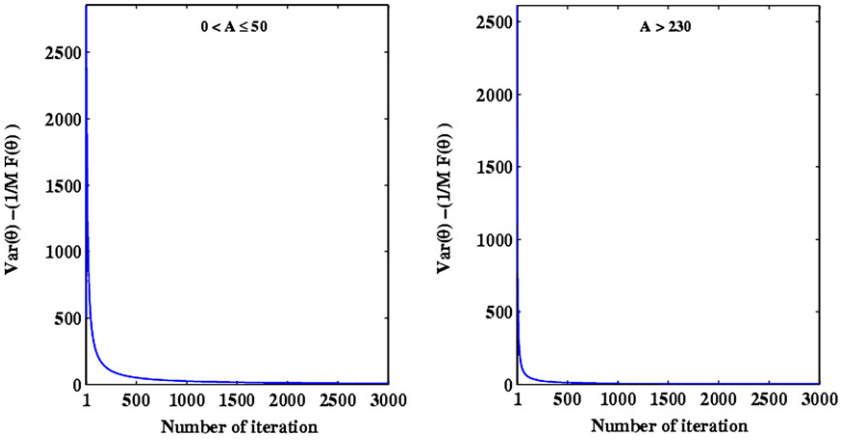

Fig. 2. (Color online.) Similar to Fig. 1, variations of CRLBs in the iteration processes for sequences prepared by nuclei taken from Table 1 of Ref. [3] classified in two mass regions ($A \leqslant 50$ and $A \geqslant 230$). Berry–Robnik distribution has employed in these estimation procedures.

of uncertainties and yield estimator's variances very close to CRLBs as shown in Figs. 1 and 2, respectively for Brody and Berry–Robnik distributions (due to similar shapes of CRLB curves, we only represent four CRLBs curves).

In Berry–Robnik distribution case, using the similar sequences have been analyzed in Ref. [18], the ML-based estimated values are obtained as the converging values of iterations (C.5) by choosing the LSF estimated values (taken from Ref. [18]) as initial values where listed in Table 3.

Table 3
Comparison of the ML estimated values of "q" in Berry–Robnik distribution with those estimated by LSF method for different sequences given in Ref. [18].

Nuclei	q (LSF-based estimated)	q (MLE-based estimated)
$A < 50$	0.03 ± 0.16	0.32 ± 0.08
$50 < A < 100$	0.27 ± 0.30	0.69 ± 0.06
$100 < A < 150$	0.37 ± 0.32	0.77 ± 0.10
$150 < A < 180$	0.53 ± 0.10	0.91 ± 0.04
$180 < A < 210$	0.27 ± 0.27	0.82 ± 0.08
$230 < A$	0.59 ± 0.18	0.95 ± 0.19
Deformed $(0^+, 3^+)$	0.29 ± 0.09	0.84 ± 0.10
Spherical $(2^+, 4^+)$	0.34 ± 0.20	0.63 ± 0.05
Deformed $(2^+, 4^+)$	0.74 ± 0.23	0.56 ± 0.21

Considering the estimated "q" values (by MLE and LSF methods) given in Tables 1–3, we can deduce the following important facts:

(I) Estimated values of both Brody and Berry–Robnik distributions parameters given in Tables 1, 3 (estimated by LSF methods), imply that, sequences prepared by lightest nuclei ($A \leqslant 50$) display more chaotic behavior in compare to heaviest ones ($230 < A$) [3]. The ML-based estimated values for both distributions suggest similar statistics but with more regular dynamics. It means, the spectra of heaviest nuclei are more regular than what LSF estimation indicates. Similarly, in light nuclei, nuclei are not so much chaotic that LSF estimation indicates.

(II) As it is predicted in Refs. [3,18] (by LSF estimation method), 2^+ and 4^+ levels are more regular (are more closer to Poisson distribution) than 0^+ and 3^+ones. Obviously, the ML estimated parameters given in Tables 2–3 confirm this but again all of above levels are more regular than what LSF indicates.

(III) The nuclei in $180 < A < 200$ mass region, i.e. spherical nuclei, are located between two sequences of deformed nuclei, namely $150 < A < 180$ and $A > 230$ ones. As it is suggested in Refs. [3,18] (by LSF estimation method), there is a considerable variations in the values of "q" which implies that, spherical nuclei exhibit more chaotic dynamics in compare to deformed ones. The ML estimated values given in Table 2 confirm this behavior but predict less chaotic dynamic for all sequences.

(IV) Similar to the predictions of Shriner et al. in Ref. [3], one expects, the spherical odd–mass and odd–odd nuclei display more chaotic dynamics in compare to deformed nuclei, the ML-based estimated values given in Tables 2 and 3 confirm this but predict less chaotic dynamic again.

(V) As already mentioned in previous sections, due to presence of noticeable uncertainties in LSF estimated values (because of high level variances of estimators), it is almost impossible to do any reliable statistical analyses of odd-odd nuclei in $50 < A < 100$ and $180 < A < 210$ mass regions [3], while as a result of small variations in the MLE method, hence minimum uncertainties, the trustworthy analysis is quite possible (see Table 2 for these reliable ML estimated "q" values for above mass region).

On the whole, the ML-based estimated values are almost exact in all sequences, even in cases with small sample sizes, where by LSF estimation method one cannot achieve the appropriate results.

Table 4
The ML-based estimated values of Berry–Robnik distribution's parameter in sequences prepared by nuclei classified in different mass regions which have definite calculated deformation parameter $\langle\beta_2\rangle$. These sequences prepared by the method introduced in Ref. [18].

Sequence	q (Berry–Robnik distribution's parameter)	$\langle\beta_2\rangle$
$A < 50$	0.32 ± 0.08	−0.025
$50 < A < 100$	0.69 ± 0.06	0.032
$100 < A < 150$	0.77 ± 0.10	0.051
$150 < A < 180$	0.91 ± 0.04	0.246
$180 < A < 210$	0.82 ± 0.08	−0.125
$230 < A$	0.95 ± 0.19	0.217

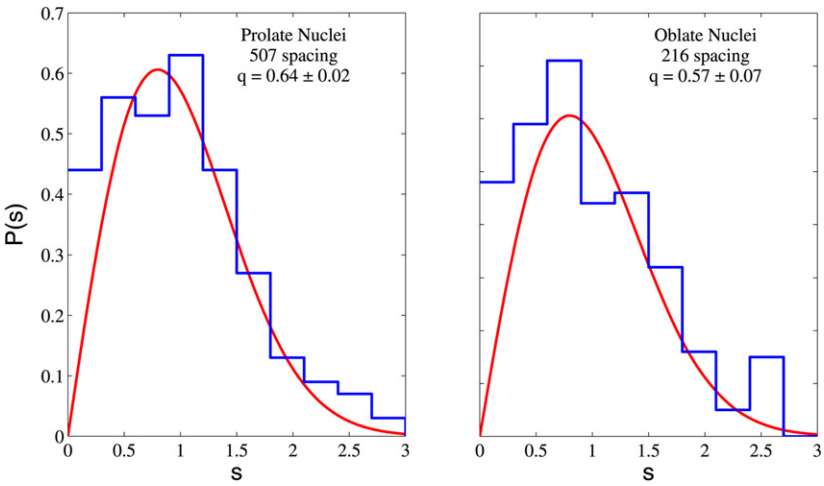

Fig. 3. (Color online.) NNS distributions for sequences prepared of oblate and prolate nuclei introduced in Ref. [20] where solid line represents ML-based estimated distribution.

Also, we can compare the ML- and LSF-based estimated values for Berry–Robnik distribution's parameter "q" in sequences prepared by nuclei with definite quadrupole deformation values. These nuclei classified in different mass region while their calculated mean deformation parameter defined as [18]

$$\langle\beta_2\rangle = \sum_k N_k \beta_2^k \Big/ \sum_k N_k,$$

where N_k represents the number of levels of nucleus k which have been involved in the analysis and β_2^k is the quadrupole deformation parameter of nucleus k taken from Ref. [25]. As it has predicted by LSF method in Ref. [18], the chaoticity degrees of sequences decrease with increasing of β. The ML-based estimated values given in Table 4, propose similar statistics but with less chaoticity degrees. Again these values are obtained as the converging values of iterations (C.5) by choosing the LSF estimated values as initial values.

In the Abul-Magd distribution case, we employed the sequences prepared by oblate and prolate nuclei introduced in Refs. [19,20] (we wouldn't review the theoretical criteria for this classification while a detailed account presented in Ref. [20]). These are the sequences have

Table 5
ML, LSF and BEM estimated values of Abul-Magd distribution's parameter "q" in sequences prepared by oblate and prolate nuclei taken from Ref. [20]. The BEM estimated values are those of Ref. [20].

Nuclei	q (obtained by LSF)	q (obtained by BEM)	q (obtained by MLE)
Prolate nuclei	0.78 ± 0.09	0.73 ± 0.05	0.64 ± 0.02
Oblate nuclei	0.61 ± 0.09	0.59 ± 0.07	0.57 ± 0.07

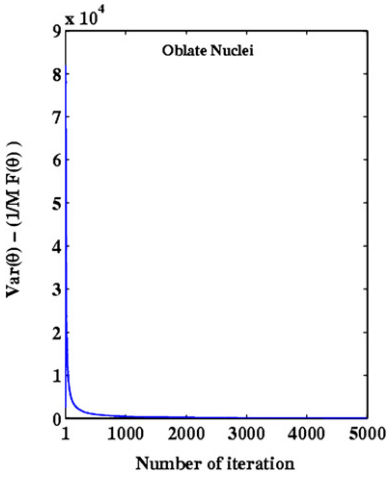

Fig. 4. (Color online.) Similar to Fig. 1, variations of CRLBs in the iteration process for sequence prepared by oblate nuclei.

been used to estimate "q", namely the parameter of Abul-Magd distribution by Bayesian estimation method (BEM) [20]. The ML-based estimated values are obtained as the converging values of iterations (D.4) where the estimated "q" values listed in Table 5 and the corresponding NNS distributions displayed in Fig. 3. For the initial values of iterations, we have chosen both LSF and BEM estimated values, where both choices yield almost the same values given in Table 5.

The above given ML-based estimated values together with NNS distributions displayed in Fig. 4, like the previous analyses [19,20], reveal some regularity in oblate sequence in compare to prolate one, but similar to other cases with less chaoticity in both sequences. With regards to the majority of oblate nuclei are deformed ones, the more regular dynamics for them may interpret as Abul-Magd–Weidenmuller [28] chaoticity effect. Also, this result suggests the weaker coupling of the single particle and collective degrees of freedom in oblate nuclei than prolate one.

Also, the ML-based estimated parameters have the least uncertainties while suggest the variances of estimators very close to CRLBs as shown in Fig. 4 (due to similarity of CRLB shapes, we only represent CRLB figure for oblate nuclei). The minimum CRLB correspond to for the final value in iteration procedure while suggested by ML estimated value. On the other hand, the LSF (or BEM) estimated values correspond to the initial values of iterations with variances far from these minimums. Therefore, one can conclude that, MLE method yield the most exact result in compare to BEM and LSF estimation methods and display less chaoticity in compare to other methods.

To analyze the spectral statistics of nuclei provide empirical evidences for three dynamical symmetry limits and transitional regions of IBM (a detailed description of these classification are

Table 6
The Nuclei provide empirical evidences for three dynamical symmetry limits and transitional regions of IBM have been used to prepare sequences.

Sequence	Nuclei
U(5)	^{98}Mo, ^{100}Mo, ^{108}Cd, ^{112}Cd, ^{114}Cd, ^{110}Cd, ^{116}Cd, ^{118}Cd, ^{118}Te, ^{120}Te, ^{122}Te, ^{124}Te, ^{126}Te, ^{112}Sn, ^{114}Sn, ^{134}Xe, ^{154}Dy
O(6)	^{56}Fe, ^{78}Ge, ^{80}Se, ^{130}Ba, ^{132}Ba, ^{132}Ce, ^{134}Ce, ^{196}Hg, ^{194}Pt, ^{196}Pt, ^{198}Pt, ^{198}Hg
SU(3)	^{166}Er, ^{176}Hf, ^{180}W, ^{168}Yb, ^{174}Hf, ^{160}Dy, ^{230}Th, ^{184}W, ^{232}Th, ^{182}W, ^{232}U, ^{178}Hf, ^{170}Yb, ^{162}Dy, ^{234}U, ^{164}Dy, ^{172}Yb, ^{240}Pu, ^{168}Er, ^{170}Er, ^{246}Cm
SU(3)–U(5)	Nd–Sm–Gd isotopes
U(5)–O(6)	Ru–Pd isotopes, Xe isotopes (else ones mentioned in the above series), ^{134}Ba
O(6)–SU(3)	Os–Pt isotopes (else ^{194}Pt, ^{196}Pt, ^{198}Pt)

Table 7
The ML- and LSF-based estimated values of Brody distribution' parameter in sequences prepared by nuclei introduced in Table 6.

Sequence	q (obtained from LSF)	q (obtained by MLE)
Nuclei with O(6) symmetry	0.52 ± 0.16	0.48 ± 0.06
Nuclei with SU(3) symmetry	0.71 ± 0.13	0.57 ± 0.08
Nuclei with U(5) symmetry	0.46 ± 0.18	0.33 ± 0.06
Nuclei with U(5)–O(6) transition	0.78 ± 0.13	0.59 ± 0.09
Nuclei with U(5)–SU(3) transition	0.74 ± 0.14	0.63 ± 0.10
Nuclei with O(6)–SU(3) transition	0.94 ± 0.14	0.74 ± 0.08

available in Refs. [29–36]), we have prepared 6 sequences of nuclei with particular symmetries listed in Table 6. In order to prepare sequences with the available empirical data taken from [21–25], we have followed the same method given in Ref. [3]. Namely, we considered nuclei in which the spin–parity J^π assignments of at least five consecutive levels are definite. In cases where the spin–parity assignments are uncertain and where the most probable value appeared in brackets, we admit this value. We terminated the sequences in each nucleus when we reach at a level with unassigned J^π. We focus on 2^+ and 4^+ levels for even mass for their relative abundance. With unfolding processes and then by using the iterations (A.4), (A.5) of corresponding estimators obtained via MLE technique, the parameter of Brody distribution estimated.

The NNSDs for these 6 sequences displayed in Fig. 5 where the ML-based estimated values listed in Table 7. Analogous to the theoretical predictions [29–31], the ML-based estimated values suggest, nuclei exhibit the U(5) (vibrational limit) dynamical symmetry explore more regularity in compare to other dynamical symmetry limits. On the other hand, nuclei in transitional regions exhibit less regular statistics in compare to dynamical symmetry limits. Again, ML technique yield estimator's variance very close to CRLB as shown in Fig. 6 for SU(3) dynamical symmetry limit and also U(5)–O(6) transitional region.

The ML-based estimated values listed in Tables 4, 5 and 7, more or less confirm the above deduced facts from the contents of Tables 1–3, namely, due to existence of noticeable uncertainties in LSF estimated values, reliable statistical analyses would be somehow impossible. On the other hand, as a result of small variations in MLE method, hence minimum uncertainties, the trustworthy analyses are possible. In general, ML estimated values are almost exact in all sequences, even in cases where one cannot reach the appropriate results by LSF or BEM estimation methods.

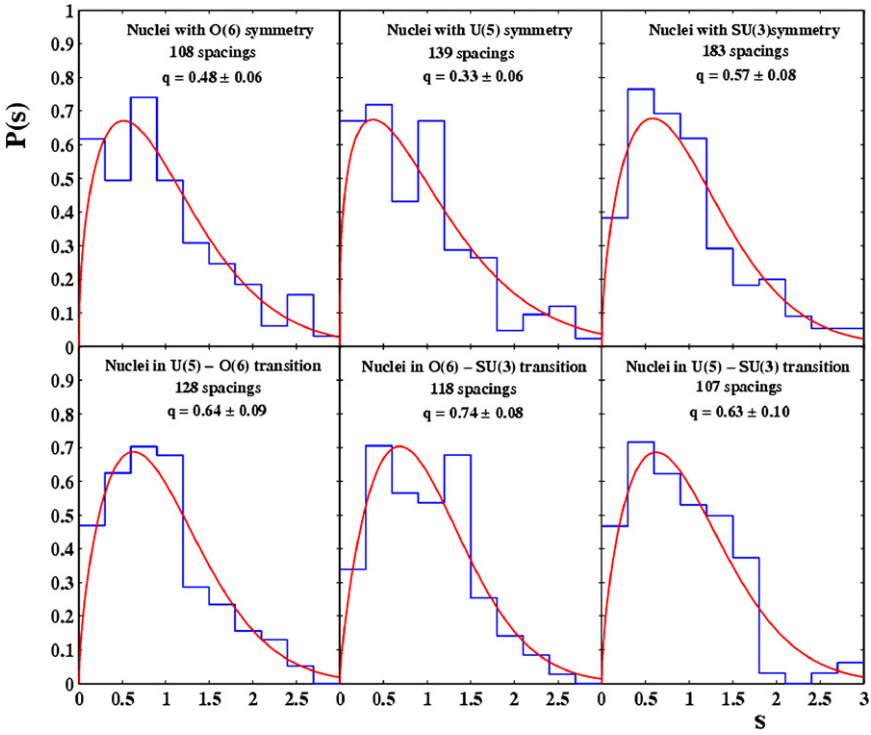

Fig. 5. (Color online.) NNS distributions for sequences prepared by nuclei provide empirical evidences for three dynamical symmetry limits and transitional regions of IBM. Solid line represents ML-based estimated distribution.

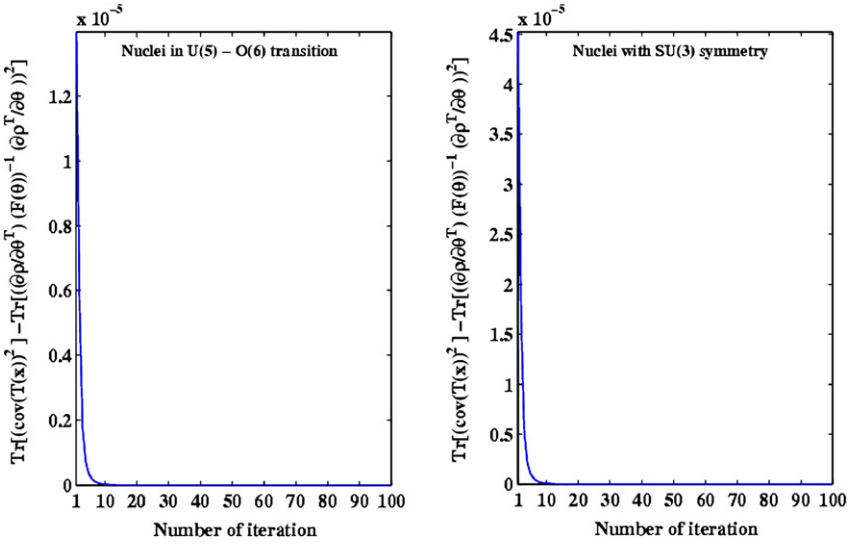

Fig. 6. (Color online.) Similar to Fig. 1, The variations of CRLBs in the iteration processes for sequences prepared by nuclei provide empirical evidences of SU(3) and U(5) ↔ O(6) transitional region.

Table 8
CRLBs for LSF-based estimated values of Brody, Berry–Robnik and Abul-Magd distributions in different sequences.

Sequence	Brody distribution	Berry–Robnik distribution	Abul-Magd distribution
Oblate nuclei	$q = 0.73$	$q = 0.37$	$q = 0.61$
	$CRLB = 0.04$	$CRLB = 0.07$	$CRLB = 0.09$
Prolate nuclei	$q = 0.82$	$q = 0.21$	$q = 0.78$
	$CRLB = 0.05$	$CRLB = 0.10$	$CRLB = 0.09$
Nuclei with U(5) symmetry	$q = 0.46$	$q = 0.44$	$q = 0.57$
	$CRLB = 0.18$	$CRLB = 0.31$	$CRLB = 0.29$
Nuclei with SU(3) symmetry	$q = 0.71$	$q = 0.31$	$q = 0.69$
	$CRLB = 0.13$	$CRLB = 0.17$	$CRLB = 0.34$
Nuclei with O(6) symmetry	$q = 0.52$	$q = 0.40$	$q = 0.62$
	$CRLB = 0.16$	$CRLB = 0.26$	$CRLB = 0.25$
Nuclei in U(5)–O(6) region	$q = 0.78$	$q = 0.22$	$q = 0.80$
	$CRLB = 0.13$	$CRLB = 0.15$	$CRLB = 0.21$
Nuclei in U(5)–SU(3) region	$q = 0.74$	$q = 0.29$	$q = 0.71$
	$CRLB = 0.14$	$CRLB = 0.18$	$CRLB = 0.31$
Nuclei in SU(3)–O(6) region	$q = 0.94$	$q = 0.19$	$q = 0.86$
	$CRLB = 0.10$	$CRLB = 0.13$	$CRLB = 0.23$

Also, the ML-based estimated values indicate less chaotic dynamics in compare to what LSF or BEM indicates.

Finally, to compare the efficiencies of considered distributions, we determined the CRLBs, namely the term defined on the right-hand side of Cramer–Rao inequality (2.12) as

$$CRLB \equiv \frac{1}{MF(\theta)}\bigg|_{\text{for final value of ``}\theta\text{'' obtained from MLE or fitting processes}}.$$

To this aim, we have evaluated the CRLBs for Brody, Berry–Robnik and Abul-Magd distributions based in sequences prepared by prolate, oblate, three dynamical symmetry and also three transitional regions of IBM (please see Appendices B–D) for details) as tabulated in Tables 8–9. The obtained result implies that, the MLE method yields good accuracies in all distributions, since the ML estimated values have the least uncertainties. It means, the variances in MLE method are closer to the CRLB than those of LSF method. Also, Brody distribution has the least CRLBs in compare to two other distributions, hence one can conclude that, it is the best NNS distribution function based on the existing theoretical and experimental data.

From these tables and figures, we see the apparent regularities and also a significant reduction of uncertainties by ML-based estimated results. Also, these results may be interpreted that nuclei provide empirical evidence for dynamical symmetries limits would be regarded as regular systems, i.e. an obvious deviation to Poisson limit occur in their spectral statistics while nuclei with mixed symmetries, namely nuclei known as candidates for transitional regions, represent less regular dynamics [29,30].

5. Conclusions

In the present paper, the spectral statistics of different nuclear systems have considered in the NNSD-based statistics. By employing the MLE technique, we have estimated the parameter of all used distributions (Brody, Berry–Robnik and Abul-Magd) in sequences prepared by nuclei classified in the different mass groups, nuclei with special values of deformation parameter (β),

Table 9
CRLBs for ML-based estimated values of Brody, Berry–Robnik and Abul-Magd distributions in different sequences.

Sequence	Brody distribution	Berry–Robnik distribution	Abul-Magd distribution
Oblate nuclei	$q = 0.60$	$q = 0.49$	$q = 0.57$
	$CRLB = 0.02$	$CRLB = 0.05$	$CRLB = 0.08$
Prolate nuclei	$q = 0.53$	$q = 0.39$	$q = 0.64$
	$CRLB = 0.03$	$CRLB = 0.07$	$CRLB = 0.06$
Nuclei with U(5) symmetry	$q = 0.33$	$q = 0.59$	$q = 0.38$
	$CRLB = 0.06$	$CRLB = 0.22$	$CRLB = 0.18$
Nuclei with SU(3) symmetry	$q = 0.57$	$q = 0.44$	$q = 0.55$
	$CRLB = 0.08$	$CRLB = 0.17$	$CRLB = 0.29$
Nuclei with O(6) symmetry	$q = 0.48$	$q = 0.43$	$q = 0.44$
	$CRLB = 0.06$	$CRLB = 0.15$	$CRLB = 0.13$
Nuclei in U(5)–O(6) region	$q = 0.59$	$q = 0.31$	$q = 0.71$
	$CRLB = 0.09$	$CRLB = 0.17$	$CRLB = 0.15$
Nuclei in U(5)–SU(3) region	$q = 0.63$	$q = 0.41$	$q = 0.62$
	$CRLB = 0.10$	$CRLB = 0.17$	$CRLB = 0.28$
Nuclei in SU(3)–O(6) region	$q = 0.74$	$q = 0.33$	$q = 0.75$
	$CRLB = 0.08$	$CRLB = 0.11$	$CRLB = 0.11$

oblate and prolate nuclei and also by nuclei provide empirical evidences for three dynamical symmetry limits and transition regions in the framework of the IBM.

In all cases, the ML-based estimated values propose minimum uncertainties in compare to those estimated by other methods, that is, the variation of ML estimated values are rather small and close enough to CRLB. Therefore, in investigating the statistical properties of nuclear spectra, MLE method is more reliable than other estimation methods, particularly LSF one. Also, the ML-based estimated values suggest more regular dynamics in compare to what LSF or BEM indicates. This is more obvious in cases with small size of data, such that LSF estimated values are not reliable at all. Finally, besides reliability, MLE method is also handier than other sophisticated estimation methods such as BEM.

Appendix A. MLE approach to Brody distribution

As mentioned in previous sections, we have employed Brody distribution by some differences (more parameter) in compare to certain distributions. This is caused by troubles which occur in maximizing the likelihood function contains Gamma functions, although we would display in the following, namely Fig. 7, a closer corresponding apparent between this definition and main distribution. For Brody distribution

$$P(s) = b(1+q)s^q e^{-bs^{q+1}}. \tag{A.1}$$

The likelihood function is assumed as

$$L(q,b) = \prod_{i=1}^{n} b(1+q)s_i^q e^{-bs_i^{q+1}} = \big[b(1+q)\big]^n \prod_{i=1}^{n} s_i^q e^{-b\sum s_i^{q+1}}. \tag{A.2}$$

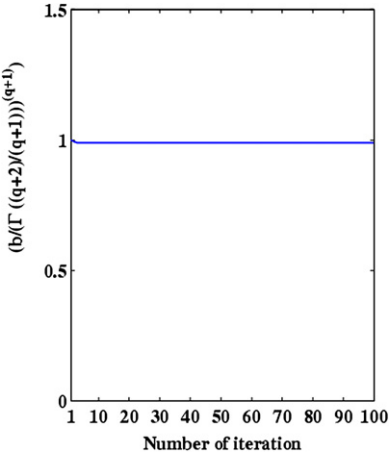

Fig. 7. (Color online.) Variation of $b/[\Gamma(\frac{2+q}{1+q})]^{q+1}$), the ratio of our proposed constant to definition of Brody distribution, in different iteration stages which verify our aim, i.e. any change wouldn't occur in compare to the main distribution.

Now, one can propose estimators as

$$\frac{\partial \ln L(q,b)}{\partial b}=0 \quad \Rightarrow \quad f_1\colon \quad \frac{1}{n}\sum s_i^{q+1}-\frac{1}{b},$$
$$\frac{\partial \ln L(q,b)}{\partial q}=0 \quad \Rightarrow \quad f_2\colon \quad \frac{b}{n}\sum \ln s_i s_i^{q+1}-\frac{1}{n}\sum \ln s_i-\frac{1}{1+q},$$

and we can achieve the final relation by using of Newton–Raphson iteration method [11]:

$$\begin{bmatrix} q_{\text{new}} \\ b_{\text{new}} \end{bmatrix}=\begin{bmatrix} q_{\text{old}} \\ b_{\text{old}} \end{bmatrix}-\mathrm{D}f^{-1}(q_{\text{old}},b_{\text{old}})f(q_{\text{old}},b_{\text{old}}), \tag{A.3}$$

$$\mathrm{D}f(q_{\text{old}},b_{\text{old}})=\begin{bmatrix} \frac{\partial f_1(q_{\text{old}},b_{\text{old}})}{\partial q} & \frac{\partial f_1(q_{\text{old}},b_{\text{old}})}{\partial b} \\ \frac{\partial f_2(q_{\text{old}},b_{\text{old}})}{\partial q} & \frac{\partial f_2(q_{\text{old}},b_{\text{old}})}{\partial b} \end{bmatrix}$$
$$=\begin{bmatrix} \frac{1}{n}\sum \ln s_i s_i^{q+1} & \frac{1}{b^2} \\ \frac{b}{n}\sum (\ln s_i)^2 s_i^{q+1}+\frac{1}{(1+q)^2} & \frac{1}{n}\sum \ln s_i s_i^{q+1} \end{bmatrix}$$

$$q_{\text{new}}=q_{\text{old}} - \frac{[\frac{1}{n}\sum \ln s_i s_i^{q_{\text{old}}+1}][\frac{1}{n}\sum s_i^{q_{\text{old}}+1}-\frac{1}{b_{\text{old}}}]-\frac{1}{b_{\text{old}}^2}[\frac{b_{\text{old}}}{n}\sum \ln s_i s_i^{q_{\text{old}}+1}-\frac{1}{n}\sum \ln s_i-\frac{1}{1+q_{\text{old}}}]}{[\frac{1}{n}\sum \ln s_i s_i^{q_{\text{old}}+1}]^2-\frac{1}{b_{\text{old}}^2}[\frac{b_{\text{old}}}{n}\sum (\ln s_i)^2 s_i^{q_{\text{old}}+1}+\frac{1}{(1+q_{\text{old}})^2}]}, \tag{A.4}$$

$$b_{\text{new}}=b_{\text{old}} - \frac{-[\frac{1}{n}\sum (\ln s_i)^2 s_i^{q_{\text{old}}+1}-\frac{1}{(1+q_{\text{old}})^2}][\frac{1}{n}\sum s_i^{q_{\text{old}}+1}-\frac{1}{b_{\text{old}}}]+[\frac{1}{n}\sum s_i s_i^{q_{\text{old}}+1}][\frac{b_{\text{old}}}{n}\sum \ln s_i s_i^{q_{\text{old}}+1}-\frac{1}{n}\sum \ln s_i-\frac{1}{1+q_{\text{old}}}]}{[\frac{1}{n}\sum s_i s_i^{q_{\text{old}}+1}]^2-\frac{1}{b_{old}^2}[\frac{b_{\text{old}}}{n}\sum (\ln s_i)^2 s_i^{q_{\text{old}}-1}+\frac{1}{(1+q_{\text{old}})^2}]}. \tag{A.5}$$

Now, if we consider the variations of $(b/[\Gamma(\frac{2+q}{1+q})]^{q+1})$, i.e. the ratio of our proposed parameter to the main definition of distribution, in the iteration processes, an exact correspondence is yield. It means, our suggestion wouldn't apply any change to main definition, as have displayed in Fig. 7.

Appendix B. CRLB of Brody distribution

As have defined in Ref. [11], the CRLB for vector function of vector parameters defined as

$$\begin{aligned}
&\mathrm{cov}_\theta\big(T(X)\big) \geqslant \frac{\partial\rho(\theta)}{\partial\theta^T}\big[F(\theta)\big]^{-1}\frac{\partial\rho^T(\theta)}{\partial\theta}, \qquad \theta_1 \to b \quad \text{and} \quad \theta_2 \to q,\\
&\rho_1 \to \frac{1}{b} \quad \Rightarrow \quad \frac{\partial\rho_1}{\partial b} = \frac{-1}{b^2},\\
&\frac{\partial\rho_1}{\partial q} = 0 \quad \text{and} \quad \rho_2 \to \frac{1}{1+q} \quad \Rightarrow \quad \frac{\partial\rho_2}{\partial b} = 0, \qquad \frac{\partial\rho_2}{\partial q} = \frac{-1}{(1+q)^2}.
\end{aligned} \tag{B.1}$$

Fisher information defined as

$$F(\theta) = \begin{bmatrix} E[(X_q - \overline{X}_q)^2] & E[(X_q - \overline{X}_q)(X_b - \overline{X}_b)] \\ E[(X_q - \overline{X}_q)(X_b - \overline{X}_b)] & E[(X_b - \overline{X}_b)^2] \end{bmatrix}, \tag{B.2}$$

where

$$\begin{aligned}
&X_b = \frac{\partial \ln L(q,b)}{\partial b} = \frac{n}{b} - \sum s_i^{q+1} \quad \text{and} \quad \bar{X}_b = \frac{1}{n}\sum X_b,\\
&X_q = \frac{\partial \ln L(q,b)}{\partial q} = \frac{n}{1+q} + \sum \ln s_i - b\sum \ln s_i s_i^{q+1} \quad \text{and} \quad \bar{X}_q = \frac{1}{n}\sum X_q.
\end{aligned} \tag{B.3}$$

The estimator functions for minimum variation are defined as

$$f_1\colon \quad q - \left(s_i^{q+1} - \frac{1}{b}\right) \quad \text{and} \quad f_2\colon \quad b - \left(b\ln s_i s_i^{q+1} - \ln s_i - \frac{1}{1+q}\right). \tag{B.4}$$

Now, with replacing the above relation in (B.1), we have

$$\mathrm{cov}_\theta\big(T(X)\big) = \begin{bmatrix} E[(f_1 - \overline{f_1})^2] & E[(f_1 - \overline{f_1})(f_2 - \overline{f_2})] \\ E[(f_1 - \overline{f_1})(f_2 - \overline{f_2})] & E[(f_2 - \overline{f_2})^2] \end{bmatrix}.$$

Consequently, the final relation to determine the CRLB for Brody distribution is prepared as

$$\begin{aligned}
&\begin{bmatrix} E[(f_1 - \overline{f_1})^2] & E[(f_1 - \overline{f_1})(f_2 - \overline{f_2})] \\ E[(f_1 - \overline{f_1})(f_2 - \overline{f_2})] & E[(f_2 - \overline{f_2})^2] \end{bmatrix}\\
&\quad \geqslant \frac{1}{E[(X_q - \overline{X}_q)^2]E[(X_b - \overline{X}_b)^2] - (E[(X_q - \overline{X}_q)(X_b - \overline{X}_b)])^2}\\
&\qquad \times \begin{bmatrix} \frac{E[(X_b - \overline{X}_b)^2]}{b^4} & -\frac{E[(X_q - \overline{X}_q)(X_b - \overline{X}_b)]}{b^2(1+q)^2} \\ -\frac{E[(X_q - \overline{X}_q)(X_b - \overline{X}_b)]}{b^2(1+q)^2} & \frac{E[(X_q - \overline{X}_q)^2]}{(1+q)^4} \end{bmatrix}.
\end{aligned} \tag{B.5}$$

Appendix C

In this section similar to Appendices A and B, we carry out the MLE-based determination for Berry–Robnik distribution

$$P(s) = \left[q + \frac{1}{2}\pi(1-q)s\right]e^{-qs - \frac{1}{4}\pi(1-q)s^2}. \tag{C.1}$$

The likelihood function is assumed as

$$L(q)=\prod_{i=1}^{n}P(s_i)=\prod_{i=1}^{n}\left[q+\frac{1}{2}\pi(1-q)s_i\right]e^{-qs_i-\frac{1}{4}\pi(1-q)s_i^2},$$
$$\ln L(q)=\sum_{i=1}^{n}\ln\left[q+\frac{1}{2}\pi(1-q)s_i\right]-\sum_{i=1}^{n}qs_i+\frac{1}{4}\pi(1-q)s_i^2. \tag{C.2}$$

Now, one can propose estimators as

$$\frac{\mathrm{d}\ln L(q)}{\mathrm{d}q}=\sum\frac{1-\frac{1}{2}\pi s_i}{q+\frac{1}{2}\pi(1-q)s_i}-\sum\left(s_i-\frac{1}{4}\pi s_i^2\right)\to F(q), \tag{C.3}$$

and by Newton–Raphson iteration method [11], we can get final result as

$$\mathrm{q}_{\mathrm{new}}=q_{\mathrm{old}}-\frac{F(q_{\mathrm{old}})}{F'(q_{\mathrm{old}})}, \tag{C.4}$$
$$q_{\mathrm{new}}=q_{\mathrm{old}}-\frac{\sum\frac{1-\frac{1}{2}\pi s_i}{q_{\mathrm{old}}+\frac{1}{2}\pi(1-q_{\mathrm{old}})s_i}-\sum s_i+\frac{1}{4}\pi s_i^2}{\sum\frac{-(1-\frac{1}{2}\pi s_i)^2}{(q_{\mathrm{old}}+\frac{1}{2}\pi(1-q_{\mathrm{old}})s_i)^2}}. \tag{C.5}$$

On the other hand, one would calculate the CRLB for Berry–Robnik distribution as

$$\mathrm{Var}(\hat{\theta})\geqslant\frac{1}{MF(\theta)},\quad \theta\to q, \tag{C.6}$$

where

$$F(\theta)=\sum\frac{1}{P(s)}\left[\frac{\mathrm{d}\ln P(s)}{\mathrm{d}\theta}\right]^2\quad\text{and}\quad M=\text{number of sample}, \tag{C.7}$$

and

$$f_1=\frac{1-\frac{1}{2}\pi s_i}{q+\frac{1}{2}\pi(1-q)s_i}\quad\text{and}\quad \mathrm{Var}(\theta)=\frac{1}{n}\sum(f_1-\overline{f}_1)^2.$$

Appendix D. Abul-Magd's distribution

$$P(s,q)=\left[1-q+q(0.7+0.3q)\frac{\pi s}{2}\right]\exp\left(-(1-q)s-q(0.7+0.3q)\frac{\pi s^2}{4}\right).$$

The likelihood function is supposed as

$$L(q)=\prod_{i=1}^{n}P(s_i)=\prod_{i=1}^{n}\left[1-q+q(0.7+0.3q)\frac{\pi s_i}{2}\right]e^{-(1-q)s_i-q(0.7+0.3q)\frac{\pi s_i^2}{4}}, \tag{D.1}$$
$$\ln L(q)=\sum_{i=1}^{n}\ln\left[1-q+q(0.7+0.3q)\frac{\pi s_i}{2}\right]-\sum_{i=1}^{n}(1-q)s_i+q(0.7+0.3q)\frac{\pi s_i^2}{4}. \tag{D.2}$$

Now, one can propose estimators as

$$\frac{\mathrm{d}\ln L(q)}{\mathrm{d}q} = \sum \frac{-1+(0.7+0.6q)\frac{\pi s_i}{2}}{\left[1-q+q(0.7+0.3q)\frac{\pi s_i}{2}\right]} + \sum s_i - (0.7+0.6q)\frac{\pi s_i^2}{4} \to F(q). \quad \text{(D.3)}$$

And we can attain the final relation by using of Newton–Raphson iteration method [11]:

$$\begin{aligned} q_{\mathrm{new}} &= q_{\mathrm{old}} - \frac{F(q_{\mathrm{old}})}{F'(q_{\mathrm{old}})} \\ &= q_{\mathrm{old}} - \frac{\sum \frac{-1+(0.7+0.6q_{\mathrm{old}})\frac{\pi s_i}{2}}{\left[1-q_{\mathrm{old}}+q_{\mathrm{old}}(0.7+0.3q_{\mathrm{old}})\frac{\pi s_i}{2}\right]} + \sum s_i - (0.7+0.6q_{\mathrm{old}})\frac{\pi s_i^2}{4}}{\sum \frac{[0.3\pi s_i][1-q_{\mathrm{old}}+q_{\mathrm{old}}(0.7+0.3q_{\mathrm{old}})\frac{\pi s_i}{2}]-[-1+(0.7+0.6q_{\mathrm{old}})\frac{\pi s_i}{2}]^2}{[1-q_{\mathrm{old}}+q_{\mathrm{old}}(0.7+0.3q_{\mathrm{old}})\frac{\pi s_i}{2}]^2} - \sum 0.15\pi s_i^2}. \end{aligned} \quad \text{(D.4)}$$

As explained for Berry–Robnik distribution, one can determine CRLB for Abul-Magd's distribution as;

$$\mathrm{Var}(\theta) \geqslant \frac{1}{MF(\theta)} \quad \theta \to q$$

where

$$F(\theta) = \sum \frac{1}{P(s)}\left[\frac{\mathrm{d}\ln P(s)}{\mathrm{d}\theta}\right]^2 \quad \text{and} \quad M = \text{number of sample} \quad \text{(D.5)}$$

and

$$f_1 = \frac{-1+(0.7+0.6q)\frac{\pi s_i}{2}}{[1-q+q(0.7+0.3q)\frac{\pi s_i}{2}]} + s_i - (0.7+0.6q)\frac{\pi s_i^2}{4} \quad \text{and}$$

$$\mathrm{Var}(\hat{\theta}) = \frac{1}{n}\sum (f_1 - \overline{f}_1)^2.$$

References

[1] M.L. Mehta, Random Matrices, 2nd ed., Academic Press, San Diego, 1991.
[2] T.A. Brody, J. Flores, J.P. French, P.A. Mello, A. Pandey, S.S.M. Wong, Rev. Mod. Phys. 53 (1981) 385.
[3] J.F. Shriner, G.E. Mitchell, T. von Egidy, Z. Phys. A 338 (1991) 309.
[4] J.F. Shriner Jr., G.E. Mitchell, E.G. Bilpuch, Z. Phys. A 332 (1989) 45;
J.F. Shriner Jr., G.E. Mitchell, E.G. Bilpuch, Phys. Rev. Lett. 59 (1987) 435;
J.F. Shriner Jr., G.E. Mitchell, E.G. Bilpuch, Phys. Rev. Lett. 59 (1987) 1492.
[5] T. von Egidy, A.N. Behkami, H.H. Schmidt, Nucl. Phys. A 481 (1988) 189;
T. von Egidy, A.N. Behkami, H.H. Schmidt, Nucl. Phys. A 454 (1986) 109.
[6] F.J. Dyson, M.L. Mehta, J. Math. Phys. 4 (1963) 701.
[7] T.A. Brody, Lett. Nuovo Cimento 7 (1973) 482.
[8] M.V. Berry, M. Robnik, J. Phys. A: Math. Gen. 17 (1984) 2413.
[9] A.Y. Abul-Magd, et al., Ann. Phys. (NY) 321 (2006) 560.
[10] A.Y. Abul-Magd, H.L. Harney, M.H. Simbel, H.A. Weidenmüller, Phys. Lett. B 579 (2004) 278.
[11] A. Van den Bos, Parameter Estimation for Scientist and Engineers, Wiley–Interscience, 2007.
[12] Hwei Piao Hsu, Schaum's Outline of Theory and Problems of Probability, Random Variables, and Random Processes, McGraw–Hill Professional, 1997.
[13] V.F. Pisarenko, D. Sornette, Phys. Rev. E 69 (2004) 036122.
[14] Kevin Judd, Phys. Rev. E 75 (2007) 036210.

[15] R.S. Asrant, Maximum likelihood estimate, Cramer–Rao lower bound and best unbiased estimate, Lecture Notes, vol. 20, May 3, 2006, http://www.wepapers.com/papers/5187/21.
[16] Murray R. Spiegel, John J. Schiller, R. Alu Srinivasan, Schaum's Outline of Theory and Problems of Probability and Statistics, McGraw–Hill Professional, 2000.
[17] Declan Mulhall, Phys. Rev. C 80 (2009) 034612;
Declan Mulhall, Phys. Rev. C 83 (2011) 054321.
[18] A.Y. Abul-Magd, M.H. Simbel, J. Phys. G: Nucl. Part. Phys. 22 (1996) 1043;
A.Y. Abul-Magd, M.H. Simbel, J. Phys. G: Nucl. Part. Phys. 24 (1998) 597.
[19] A. Al-Sayed, J. Stat. Mech. (2009) P02062.
[20] A.Y. Abul-Magd, A.A.L. Sayed, Phys. Rev. C 74 (2006) 037301.
[21] National Nuclear Data Center, Brookhaven National Laboratory, Chart of nuclides, http://www.nndc.bnl.gov/chart/reColor.jsp?newColor=dm.
[22] Live chart, Table of nuclides, http://www-nds.iaea.org/relnsd/vcharthtml/VChartHTML.html.
[23] Richard B. Firestone, Virginia S. Shirley, S.Y. Frank, Coral M. Baglin, Jean Zipkin, Table of Isotopes, 1996.
[24] Nuclear Data Tables up to 2011.
[25] P. Möller, J.R. Nix, W.D. Myers, W.J. Swiatecki, At. Data Nucl. Data Tables 59 (1995) 185.
[26] F. Iachello, A. Arima, The Interacting Boson Model, Cambridge Univ. Press, Cambridge, 1987.
[27] P. Cejnar, J. Jolie, R.F. Casten, Rev. Mod. Phys. 82 (2010) 2155.
[28] V. Paar, D. Vorkapic, Phys. Lett. B 205 (1988) 7;
V. Paar, D. Vorkapic, Phys. Rev. C 41 (1990) 2397.
[29] Y. Alhassid, A. Novoselsky, Phys. Rev. C 45 (1992) 1677.
[30] Y. Alhassid, N. Whelan, Phys. Rev. Lett. 67 (1991) 816;
Y. Alhassid, N. Whelan, Nucl. Phys. A 556 (1993) 42.
[31] A.Y. Abul-Magd, S.A. Mazen, M. Abdel-Mageed, A. Al-Sayed, Nucl. Phys. A 839 (2010) 1.
[32] R. Fossion, C. De Coster, J.E. García-Ramos, T. Werner, K. Heyde, Nucl. Phys. A 697 (2002) 703.
[33] J.E. Garcia-Ramos, C. De Coster, R. Fossion, K. Heyde, Nucl. Phys. A 688 (2001) 735.
[34] Jing Shu, Ying Ran, Tao Ji, Yu-xin Liu, Phys. Rev. C 67 (2003) 044304.
[35] Zhan-feng Hou, Yu Zhang, Yu-xin Liu, Phys. Rev. C 80 (2009) 054308.
[36] F. Iachello, Phys. Rev. Lett. 87 (2001) 052502.